

Semi-Supervised Learning Approach for Efficient Resource Allocation with Network Slicing in O-RAN

Salar Nouri[†] Mojdeh Karbalaee Motalleb[†] Vahid Shah-Mansouri[†] Seyed Pooya Shariatpanahi[†]

[†] School of Electrical and Computer Engineering, College of Engineering, University of Tehran, Tehran, Iran
 {salar.nouri, mojdeh.karbalaee, vmansouri, p.shariatpanahi}@ut.ac.ir

Abstract—The Open Radio Access Network (O-RAN) technology has emerged as a promising solution for network operators, providing them with an open and favorable environment. Ensuring effective coordination of x-applications (xAPPs) is crucial to enhance flexibility and optimize network performance within the O-RAN. In this paper, we introduce an innovative approach to the resource allocation problem, aiming to coordinate multiple independent xAPPs for network slicing and resource allocation in O-RAN. Our proposed method focuses on maximizing the weighted throughput among user equipments (UE), as well as allocating physical resource blocks (PRBs). We prioritize two service types, namely enhanced Mobile Broadband and Ultra Reliable Low Latency Communication. To achieve this, we have designed two xAPPs: a power control xAPP for each UE and a PRB allocation xAPP. The proposed method consists of a two-part training phase, where the first part uses supervised learning with a Variational Autoencoder trained to regress the power transmission as well as the user association and PRB allocation decisions, and the second part uses unsupervised learning with a contrastive loss approach to improve the generalization and robustness of the model. We evaluate the performance of our proposed method by comparing its results to those obtained from an exhaustive search algorithm, deep Q-network algorithm, and by reporting performance metrics for the regression task. We also evaluate the proposed model's performance in different scenarios among the service types. The results show that the proposed method is a more efficient and effective solution for network slicing problems compared to state-of-the-art methods.

Index Terms—Resource allocation, Network slicing, O-RAN, Variational Autoencoder, Contrastive Learning

I. INTRODUCTION

Wireless communication has evolved from a mere convenience to an absolute necessity, driven by an insatiable demand for faster and more dependable connectivity between various quality of service (QoS) requirements [1]. The emergence of fifth generation (5G) technology represents a significant leap, offering the potential to support a wide range of applications, including augmented reality and autonomous vehicles [2]. However, the pursuit of wireless excellence does not conclude with 5G; it merely marks a stepping stone towards the next frontier—sixth generation (6G), the sixth generation of wireless technology. Poised on the horizon, 6G holds the promise to once again redefine the boundaries of connectivity.

Emerging concepts within 6G, such as extreme Multiple-Input Multiple-Output and deep Receiver, promise to propel

us further into uncharted technological realms, offering unprecedented data rates and levels of connectivity [3]. These advancements have the potential to not only revolutionize our modes of communication but also reshape the very fabric of our interconnected world. Furthermore, the application of various machine learning (ML) techniques to automate resource allocation within the medium access control (MAC) layer and scheduler represents a burgeoning area of research within the 6G landscape [4]. These techniques aim to inject an unparalleled level of intelligence into network management and optimization, laying the foundation for networks capable of dynamically adapting to user demands and environmental conditions.

In this constantly evolving landscape, the roles of Open Radio Access Network (O-RAN) [5] and network slicing [6], which have reached remarkable milestones in 5G, continue to be pivotal. As we explore the possibilities offered by 6G and its transformative capabilities, it becomes increasingly evident that the evolution of wireless communication is an unceasing journey. Each generation builds upon the accomplishments of its forerunners, establishing a robust foundation for the next phase of wireless excellence.

Resource allocation involves the meticulous distribution of finite network resources among numerous users, applications, or services [7]. In 5G, the primary objective is to support a wide spectrum of services, including Enhanced Mobile Broadband (eMBB), Ultra-Reliable Low Latency Communications (URLLC), and massive Machine Type Communications (mMTC) [8]. Each of these services necessitates distinct resource sets encompassing bandwidth, data rate, latency, power consumption, complexity, and reliability. As such, resource allocation within the 5G landscape must exhibit the flexibility to cater to these diverse demands while ensuring the efficient utilization of network resources.

Network slicing is an innovative concept that tailors virtual networks (slices) within a unified physical infrastructure, addressing specific service types and use cases [9]. In the context of 5G, it efficiently allocates resources for eMBB and URLLC [10] services. This significance extends into the anticipated 6G era, where network slicing remains instrumental, facilitating resource allocation for diverse applications, including holographic communication and tactile internet [11], [12]. Its inherent scalability ensures adaptability to evolving workloads and user expectations, solidifying its role as a key technology

in the relentless pursuit of wireless excellence, bridging the transition from 5G to 6G.

This concept seamlessly aligns with the architecture of the O-RAN. O-RAN is based on open interfaces, open hardware, and open software and aims to provide a more flexible and cost-effective solution for wireless communication [7]. Within this context, the implementation of network slicing in O-RAN not only optimizes resource allocation but also fosters multi-vendor interoperability and innovation.

At the core of O-RAN's architecture are two fundamental components: Radio Units (RUs), responsible for physical layer functions, and Distributed Units (DUs), which manage base-band processing and control. These components collaborate seamlessly, with the Central Unit (CU) serving as a centralized coordinator for network resources, facilitating dynamic resource allocation [5], [13]. The CU further comprises two distinct elements: the control plane (CP) and the user plane (UP). Adding to O-RAN's adaptability and innovation are xApps (cross-applications), capable of spanning multiple network domains to optimize resource allocation for various services. These network segments include Fronthaul, Backhaul, and Midhaul, facilitating data transmission between components. Overseeing resource management and orchestration tasks is the Management and Orchestration (MANO) layer, ensuring the network's efficiency. Network Functions Virtualization (NFV) decouples software from hardware, enhancing scalability. Furthermore, the Radio Access Network Intelligent Controller (RIC) plays a pivotal role in intelligent resource control, enabling dynamic allocation to meet diverse service requirements [5]. These components collectively define O-RAN's transformative architecture, promoting openness, adaptability, and efficient resource utilization in modern wireless networks. It is worth noting that O-RAN comprises two types of RIC: near-real-time (near-RT) RIC, which manages Radio Access Network (RAN) control and optimization, and non-real-time (non-RT) RIC. Within the near-RT RIC, xAPPs facilitate RAN control and optimization, while inside the non-RT RIC, rAPPs support it by providing guidance and employing ML models. Furthermore, both xAPPs and rAPPs can be implemented by third-party entities, allowing for a diverse ecosystem of applications within the O-RAN architecture [14].

Moreover, xAPPs leverage O-RAN network slicing for efficient resource utilization, allowing seamless collaboration across services. However, this introduces network management complexity, as each xAPP must adapt to multiple slice QoS needs, posing a critical coordination challenge. Additionally, cellular operators face the difficulty of establishing consistent connectivity for devices with different QoS demands [15], [16]. Therefore, in this study, we examine the resource allocation problem using network slicing by considering the xAPPs. We propose a novel method for resource allocation, with the goal of effectively coordinating numerous independent xAPPs to address the network slicing and resource allocation challenges within O-RAN.

The application of ML algorithms in wireless networks has surged due to the escalating complexity of these networks and the challenges posed by crafting custom optimization models. Traditional approaches, such as convex/non-

convex optimization, are grappling with mounting complexity stemming from shifts in network architecture, evolving performance requirements, and the proliferation of devices. Present methods for network resource allocation that rely on learning-based techniques, like deep learning (DL) and deep reinforcement learning (DRL), often neglect the capacity to learn resource distributions. Typically, these methods involve designing an agent for a specific task and training it from scratch, resulting in reduced exploration efficiency and extended convergence times. Moreover, they necessitate a substantial volume of training samples, leading to prolonged exploration phases. The limited adaptability of traditional ML methods to novel scenarios motivates us to explore an alternative approach capable of superior generalization, more efficient data utilization, and resource distribution learning. To address these objectives, we propose a novel methodology that employs a self-supervised learning technique, specifically contrastive learning [17], in conjunction with a variational autoencoder (VAE) model, known as a type of generative model [18]. These models excel in handling uncertainty by learning potential outcome distributions, thereby offering a distribution of predictions instead of a singular deterministic output. Moreover, their adeptness in handling incomplete or missing data allows for the imputation of missed values based on learned data patterns. VAEs also exhibit proficiency in semi-supervised learning setups, effectively harnessing both labeled and unlabeled data to enhance predictive accuracy. Their generative abilities facilitate the creation of new data instances resembling the training set, proving beneficial in scenarios demanding synthetic data generation or heightened resilience against noise and outliers.

Furthermore, contrastive learning involves contrasting different examples to acquire informative data representations. On the other hand, a VAE comprises an encoder and decoder that jointly learn the underlying probability distribution of data. By integrating contrastive learning with VAE, we can mitigate the common challenge of requiring a large number of training samples in ML. This approach can enhance performance metrics, such as quicker convergence and improved results, while also reducing the time and effort needed for algorithm design and training.

A. Contribution

This paper introduces a system model within the O-RAN architecture that provides support for two primary services, namely eMBB and URLLC, through resource allocation, with a particular emphasis on network slicing.

Our paper's primary contributions can be summarized as follows:

- Our research primarily aims to tackle resource allocation challenges in the O-RAN architecture, with a specific focus on optimizing weighted throughput by allocating resources like transmission power and physical resource blocks. We account for the unique QoS requirements and service priorities of two key 5G services: eMBB and URLLC. Compared to existing joint resource allocation schemes, our xAPP-based architecture enhances network management flexibility.

- Our solution to the resource allocation optimization problem employs a two-step algorithm. Firstly, we simplify the problem by framing it as an optimization task. Secondly, we employ a two-phase training approach. We use supervised learning with a VAE to train power transmission regression and resource allocation decisions. This is followed by unsupervised learning with a contrastive loss method to enhance the model's generalization and robustness. In essence, our approach simultaneously handles power and radio resource allocation xAPPs. In addition, it is not limited to O-RAN but can be applied to future multi-vendor O-RAN architectures, leveraging team learning principles developed by our team.

B. Structure of Paper

The paper is structured as follows: Section II presents a review of related works. In Section III, we introduce the system model for the resource allocation problem in the O-RAN architecture and formally define the resource allocation problem as an optimization problem. Section IV provides a detailed description of the proposed resource allocation algorithm. In Section V, we present numerical results used to evaluate the algorithm's performance. Finally, Section VI offers our conclusion.

II. RELATED WORKS

As mentioned in Section I, cellular operators face significant challenges in ensuring reliable connections for devices with diverse QoS requirements. This challenge becomes more pronounced in 5G networks due to their increased complexity and stringent QoS demands [16]. Recently, there has been a growing focus on addressing the network slicing problem in cellular networks, as evidenced by several studies [16], [19]–[22].

Feng et al. [16] proposed a method that employs network slicing and scheduling to allocate resources based on QoS requirements. However, their simulation utilized only a limited number of User Equipment (UE) devices and service types, which may not accurately represent real-world 5G networks with diverse service requirements. In another study, a resource allocation approach based on the M/M/1 queuing system was presented for RAN slicing [19]. Nevertheless, practical scenarios often involve bursty traffic, rendering the M/M/1 assumption of a Poisson distribution of packet arrivals at each gNodeB, which serves the eMBB and URLLC services, overly optimistic. Consequently, the gNodeB cannot be considered an M/M/1 system, and its queue cannot be accurately modeled as a continuous-time Markov process. Additionally, in a study by Kazemifard et al. [20], an O-RAN system was investigated, assuming that the core network and RAN are co-located in the same data center. The authors conducted a theoretical analysis and employed a mathematical model to efficiently address minimum delay problems.

Various approaches have been proposed in the literature to address resource allocation challenges in wireless networks, including optimization techniques, game theory, and ML algorithms [23]. ML algorithms, in particular, have found

application in power control and resource allocation within wireless networks. These models are trained on historical resource allocation decisions and then applied to make new allocation decisions.

For instance, the SAMUS framework was employed by Bektas et al. [24] to forecast incoming traffic, enabling an exploration of various network slicing operations and a discussion of the trade-off between the data rate of eMBB and the latency of URLLC. Li et al. [25] introduced a method that utilizes DRL for proactive resource allocation to mobile UE, considering both time and frequency domains while accounting for mobility. Wu et al. [26] proposed a dynamic resource allocation method for radio and computation resources through RAN slicing, including a defined learning scheme with constraints.

Further, Ayala et al. [27] presented a method for the joint allocation of virtualized RAN's radio and computation resources using a DRL approach based on an actor-critic network. Wang et al. [28] introduced a DRL-based self-play approach that can be integrated into RAN architecture to efficiently manage RU and DU resources, leading to cost-effective RAN operations. In another approach, Ndikumana et al. [29] combined federated learning and Deep Q-Learning with a reward function to reduce offloading, fronthaul routing, and computation delays in O-RAN.

Similarly, Samarakoon et al. [30] introduced a federated learning algorithm to optimize transmit power and radio resource allocation in vehicular networks. Additionally, Elsayed et al. [31] proposed a reinforcement learning-based method for joint power and radio resource allocation in 5G networks.

III. SYSTEM MODEL AND PROBLEM FORMULATION

In our study, we address network slicing and resource allocation problem within O-RAN architecture, focusing on two primary slices: the URLLC slice and the eMBB slice. The URLLC slices ensure ultra-low latency and high reliability for critical applications such as autonomous driving and remote surgery, while eMBB slices focus on high data rates for mobile broadband. These slices have also various QoS requirements for network resource allocation [10].

By slicing the RAN into dedicated components for URLLC and eMBB, we can tailor network optimization to distinct traffic types and services, enhancing the efficient and flexible utilization of network resources. Key resources in O-RAN allocation encompass transmission power and Physical Resource Blockss (PRBs). Traffic demands, often quantified by data rate and bandwidth, reflect the volume of data requiring transmission through the network. QoS requirements delineate the desired network performance based on parameters such as data rate. Our system model for resource allocation with network slicing is illustrated in Fig. 1.

In our study, we investigate an O-RAN-based deployment, wherein each base station, known as RU in O-RAN, accommodates two distinct slices: eMBB and URLLC. These slices cater to UEs with comparable QoS requirements. Our analysis encompasses two critical network functions: power control and radio resource allocation, which are jointly considered. We

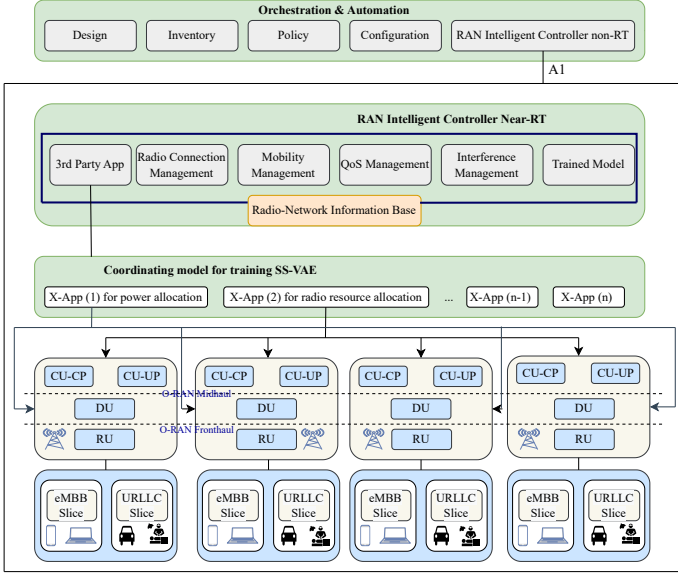


Fig. 1: O-RAN network system model

denote the set of all RUs as \mathcal{B} and the set of UEs as \mathcal{U} . Each base station b serves two sets of users: $\mathcal{U}_{e,b}$ for eMBB and $\mathcal{U}_{u,b}$ for URLLC, leading to a total of U users, where $U = U_{e,b} + U_{u,b}$. Each user is exclusively associated with a single RU. The temporal and spectral layout is partitioned into \mathcal{M} segments referred to as PRBs. These PRBs constitute the smallest unit of resources for allocation [32]. Each PRB spans a time frame, defined as a time slot in the temporal domain, and covers a frequency range of f Hz in the spectral domain. We also denote S_e for eMBB slices and S_u for URLLC slices. The total number of slices (S) will be: $S = S_e + S_u$.

The user association is indicated by a binary variable $\alpha_{u,b,s}$, which takes a value of 1 if user u is connected to RU b in slice s , and 0 if not. Since each UE should be connected to only one RU, the following constraint must be met:

$$\sum_{b \in \mathcal{B}} \alpha_{u,b,s} = 1 \quad \forall u \in \mathcal{U}, \quad s \in \mathcal{S}. \quad (1)$$

We define the binary variable $\beta_{u,b,m,s}$ as the indicator for PRB allocation, taking the value of 1 when user u in slice s is connected to PRB m of RU b , and 0 otherwise.

$$\beta_{u,b,m,s} \leq \alpha_{u,b,s} \quad \forall b \in \mathcal{B}, \quad m \in \mathcal{M}, \quad u \in \mathcal{U}, \quad s \in \mathcal{S}. \quad (2)$$

Similarly, each PRB m of RU b should be associated with only one UE, as defined below:

$$\sum_{u \in \mathcal{U}} \alpha_{u,b,s} \beta_{u,b,m,s} \leq 1 \quad \forall b \in \mathcal{B}, \quad m \in \mathcal{M}, \quad s \in \mathcal{S}. \quad (3)$$

The rate achieved for a user u by allocating PRB m of RU b is denoted by $R_{u,b,m,s}$, where $\eta_{u,b,m,s}$ represents the Signal to Interference & Noise Ratio (SINR). The calculation for $R_{u,b,m,s}$ is determined by:

$$\eta_{u,b,m,s} = \frac{\alpha_{u,b,s} h_{u,b,m,s} p_{u,b,m,s}}{\sum_{j \neq b} \sum_{l \neq s} \sum_{i \neq u} \alpha_{i,j,l} h_{i,j,m,l} p_{i,j,m,l} + \sigma^2}, \quad (4)$$

$$R_{u,b,m,s} = \log_2(1 + \eta_{u,b,m,s}), \quad (5)$$

$$R_{u,s} = \sum_{b \in \mathcal{B}} \sum_{m \in \mathcal{M}} \alpha_{u,b,s} \beta_{u,b,m,s} R_{u,b,m,s}, \quad (6)$$

$$\begin{aligned} R_u &= \sum_{s \in \mathcal{S}} \sum_{u \in \mathcal{U}} \alpha_{u,b,m,s} \sum_{m \in \mathcal{M}} \beta_{u,b,m,s} R_{u,b,m,s} \\ &= \sum_{u \in \mathcal{U}} \sum_{m \in \mathcal{M}} \beta_{u,b,m} R_{u,b,m,s} \quad \forall m \in \mathcal{M}, \quad s \in \mathcal{S}. \end{aligned} \quad (7)$$

The total power transmitted by RU b and the data rate for UE in the fronthaul link are represented as P_b and C_b , respectively. The existence of quantization noise (σ_1^2) can potentially impact the signal's fidelity during transmission over the fronthaul, particularly when the original signal displays significant variations or spans a wide range of values. This noise may lead to inaccuracies in the transmitted signal, thereby influencing the QoS perceived by the UE. These values are determined as follows:

$$P_b = \sum_{u=1}^U \sum_{m=1}^M \sum_{s=1}^S \alpha_{u,b,s} h_{u,b,m,s} p_{u,b,m,s} + \sigma_1^2, \quad (8)$$

$$\begin{aligned} C_b &= \log_2 \left(1 + \frac{\sum_{u=1}^U \sum_{m=1}^M \sum_{s=1}^S \alpha_{u,b,s} h_{u,b,m,s} p_{u,b,m,s}}{\sigma_1^2} \right) \\ &= \log_2 \left(\frac{P_b}{\sigma_1^2} \right), \end{aligned} \quad (9)$$

where, we denote the transmission power of PRB m in RU b in slice s as $p_{u,b,m,s}$ for UE u , and the channel gain between RU b and UE u in slice s as $h_{u,b,m,s}$. Furthermore, we define the channel gain between the resources and UE as h_{ij} . To represent this relationship in matrix form, we construct a matrix that accounts for \mathcal{B} resources and \mathcal{U} users as follows:

$$H := \begin{bmatrix} |H_{11}|^2 & \cdots & |H_{1U}|^2 \\ \vdots & \vdots & \vdots \\ |H_{B1}|^2 & \cdots & |H_{BU}|^2 \end{bmatrix}_{B \times U} \quad (10)$$

The overall propagation delay (D^{pro}) comprises three distinct components: the propagation delay in the fronthaul link ($D^{fr,p}$), the midhaul link ($D^{mid,p}$), and the backhaul link ($D^{b,p}$). In each of these links, the propagation delay is determined by the time it takes for a signal to traverse the distance, calculated as $D = \frac{L}{C}$, where L signifies the length of the fiber link, and C represents the propagation speed of the medium.

Similarly, the total transmission delay (D^{tr}) is the aggregate of transmission delays in the fronthaul ($D^{fr,t}$), midhaul ($D^{mid,t}$), and backhaul ($D^{b,t}$) links. Within each link, the transmission delay corresponds to the time needed to transmit all packets into the transmission medium, represented as

$D = \frac{\alpha}{R}$, where R indicates the data rate of the packet, and α denotes the mean packet size.

$$D_{total} = D^{pro} + D^{tr}, \quad (11)$$

$$D_{u,s} = \frac{L}{C} + \frac{\alpha}{R_{u,s}}. \quad (12)$$

Therefore, the delay of UE u in slice s , as derived from Equation 12, should be constrained to be below a specific threshold relevant to its respective slice, outlined below:

$$D_{u,s} \leq D_{u,s}^{min}. \quad (13)$$

The objective function is designed to optimize the overall network utility, which involves maximizing the weighted sum of the data rates achieved by UEs while ensuring compliance with QoS requirements. In this context, w_s signifies the priority associated with individual service types and UEs. The intelligent RU is responsible for effectively managing the requirements of both network slices. Hence, we can mathematically express the problem in the following manner:

$$\max_{\mathbf{p}, \alpha, \beta} \sum_{s \in \mathcal{S}} \sum_{u \in \mathcal{U}} w_s R_{u,s} \quad (14)$$

subject to

$$P_b \leq P_b^{max} \quad \forall b \in \mathcal{B} \quad (15)$$

$$p_{u,b,m,s} \geq 0 \quad \forall b \in \mathcal{B}, m \in \mathcal{M}, s \in \mathcal{S}, u \in \mathcal{U} \quad (16)$$

$$p_{u,b,m,s} \leq P_s^{max} \quad \forall b \in \mathcal{B}, m \in \mathcal{M}, s \in \mathcal{S}, u \in \mathcal{U} \quad (17)$$

$$R_{u,s} \geq R_s^{max} \quad \forall u \in \mathcal{U}, s \in \mathcal{S} \quad (18)$$

$$C_b \leq C_b^{max} \quad \forall b \in \mathcal{B} \quad (19)$$

$$D_{u,s} \leq D_{u,s}^{min} \quad \forall u \in \mathcal{U}, s \in \mathcal{S}, \quad (20)$$

$$\alpha_{u,b,s} \in \{0, 1\} \quad \forall u \in \mathcal{U}, b \in \mathcal{B}, s \in \mathcal{S} \quad (21)$$

$$\beta_{u,b,m,s} \in \{0, 1\} \quad \forall u \in \mathcal{U}, b \in \mathcal{B}, m \in \mathcal{M}, s \in \mathcal{S} \quad (22)$$

$$\sum_{b \in \mathcal{B}} \alpha_{u,b,s} = 1 \quad \forall u \in \mathcal{U}, s \in \mathcal{S} \quad (23)$$

$$\beta_{u,b,m,s} \leq \alpha_{u,b,s} \quad \forall b \in \mathcal{B}, m \in \mathcal{M}, u \in \mathcal{U}, s \in \mathcal{S} \quad (24)$$

$$\sum_{u \in \mathcal{U}} \alpha_{u,b,s} \beta_{u,b,m,s} \leq 1 \quad \forall b \in \mathcal{B}, m \in \mathcal{M}, s \in \mathcal{S} \quad (25)$$

IV. METHODOLOGY

Our primary focus is to address resource allocation problem within O-RAN architecture, and we propose a novel approach based on semi-supervised learning. Our objective is to optimize the sum of rates among UEs while considering constraints, including transmission power and PRB allocation. To accomplish this, we compile a dataset comprising diverse resource allocation scenarios, encompassing various combinations of objective functions and constraints. We generate this dataset using an exhaustive search algorithm (ESA), which explores the entire feasible solution space.

Our research primarily delves into the resource allocation problem within the O-RAN architecture, and we introduce an innovative approach based on semi-supervised learning.

Our primary goal is to enhance the cumulative rates for UEs while adhering to specific constraints such as transmission power, delay, and PRB allocation. To achieve this, we curate a comprehensive dataset that encompasses a wide range of resource allocation scenarios, covering diverse combinations of objective functions and constraints. This dataset is generated through the implementation of an ESA, which thoroughly explores the entire feasible solution space.

In our approach to addressing the resource allocation problem, we employ a deep neural network (DNN) model integrated with a contrastive loss function. This DNN model efficiently manages the complexities of resource allocation and acquires the ability to map input features to resource allocation decisions. Through the training of our model on the dataset we've created, we fine-tune it to estimate resource allocation decisions that fulfill the requirements of the optimization problem. This semi-supervised learning algorithm, which combines a VAE with a contrastive loss, is denoted as "SS-VAE."

We aim to evaluate the performance of our learning-based approach using multiple regression-based performance metrics to assess its robustness. Additionally, we will validate the effectiveness of our model by comparing its outcomes with those of the ESA in different scenarios. Moreover, while the ESA is the optimal algorithm for resource allocation decisions, its complexity makes it impractical for deployment in real-world environments. Therefore, we will also compare the performance of our proposed algorithm with state-of-the-art methods known for their practical deployment capabilities, such as DRL. This comprehensive assessment will demonstrate the method's reliability across diverse scenarios.

Fig. 2 illustrates the overview of our proposed methodology for training the SS-VAE and comparing its results with those of the benchmark algorithms.

A. Exhaustive Search Algorithm

The ESA is a well-established optimization approach for solving resource allocation problems in wireless networks. Its fundamental concept involves generating all possible resource allocation combinations and selecting the best one based on a predefined objective function [33]. ESA serves as a valuable benchmark solution, providing a ground truth against which results from other methods can be validated and compared. Its advantages include simplicity of understanding and implementation, along with the assurance of yielding an optimal solution within a finite time frame.

Nonetheless, ESA's primary limitation lies in its computational complexity, especially when addressing resource allocation problems with extensive dimensions and intricate constraints. The computational burden grows exponentially with the size of the problem, rendering ESA impractical for large-scale resource allocation tasks [34]. Despite this drawback, ESA remains a popular choice as a baseline for comparing various optimization algorithms and offers a crucial reference for evaluating new optimization strategies.

To assess the performance, validity, and robustness of the proposed learning-based method, we will compare its results with those generated by ESA. Additionally, a subset of solu-

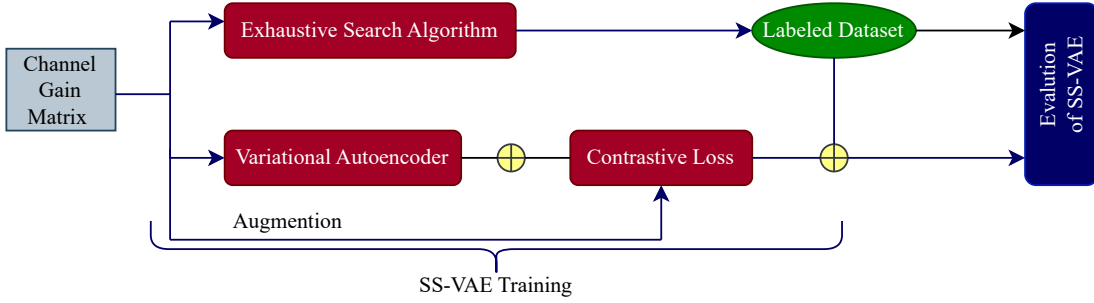


Fig. 2: The overview of proposed methodology.

tions for the resource allocation and network slicing optimization problem within O-RAN will be generated using ESA. This labeled dataset will be utilized to train the supervised learning component of the proposed method.

B. Deep Reinforcement learning Algorithm

As discussed in Section II, DRL algorithms have proven to be effective solutions for addressing resource allocation problems. These algorithms have been successfully deployed in various real-world wireless network environments, demonstrating their practicality and their ability to significantly improve both technical and business metrics [35]. Consequently, we utilize DRL, where an agent interacts with the environment to make resource allocation decisions and receive related rewards. These rewards are tied to the objective function outlined in Problem 14, considering its objectives and constraints. Next, we model the problem as a Markov Decision Process (MDP) and introduce the DRL algorithm to address the resource allocation challenge in network slicing. This approach serves as an extra means to evaluate the robustness and our primary proposed solution.

1) *Markov Decision Process*: In the specified resource allocation problem (Equation 14), an O-RAN orchestrator is responsible for determining PRB allocation decisions and determine the corresponding RU for each UE for entw. This problem can be represented as a MDP denoted by $(\mathfrak{S}, \mathfrak{A}, \mathfrak{P}, \mathfrak{R})$, where \mathfrak{S} represents the state space, \mathfrak{A} is the action space, $\mathfrak{P}(s'|s, a)$ signifies the transition probability from state s to state s' by taking action a , and \mathfrak{R} represents the reward function [35]–[38], which are elaborated for our specific problem.

I. **State**: The state at time t ($s(t) \in \mathfrak{S}$), is represented by $\{\mathfrak{s}_u(t)\}_{t=1}^N$, where $\mathfrak{s}_u(t)$ indicates the state of UE u ($u = 1 : U$). Here, $\mathfrak{s}_u(t)$ is a binary indicator: it equals 1 if the data rate requirement of UE u is met and 0 otherwise. It's important to note that each data rate corresponds to a specific transmission power level.

II. **Action**: An action ($a \in \mathfrak{A}$), is represented as $a = \{\alpha_{u,b,s}, \{\beta_{u,b,m,s}\}_{m=1}^M\}_{b=1}^B$.

III. **Transition Probability**: The transition probability $\mathfrak{P}(s'|s, a)$ represents the probability of moving from one state s to another one s' by taking action a . It is influenced by several factors, including the QoS requirements of UEs and the resource allocation decisions made for UEs.

IV. **Reward**: The reward function serves as a pivotal element in assessing the gains or expenses associated with a given state-action pair. It provides guidance to the agent's decision-making process, indicating the appeal of different actions across various states. In alignment with earlier studies [35]–[37], our method characterizes the reward function as a combination of the objective function and the constraints relevant to the considered problem (14). Therefore, we establish the reward function for our specific problem as follows:

$$\mathfrak{R}(s, a) = \Theta_r R_{u,s} + \Theta_{const.} C_{u,b,m,s} + \Theta_{bias}, \quad (26)$$

where, Θ_r , $\Theta_{const.}$, and Θ_{bias} represent the respective weights assigned to the objective function (Data Rate), constraints, and the bias value.

The primary objective of the agent is to determine the optimal policy, denoted as $\pi : \mathfrak{S} \rightarrow \mathfrak{P}(\mathfrak{A})$, for the MDP. This policy maps any state $s \in \mathfrak{S}$ to a probability distribution $\pi(\cdot|s)$ over the set of possible actions \mathfrak{A} . The goal is to find a policy that maximizes the cumulative reward obtained through dynamic learning from acquired data. The policy π can be influenced and controlled by decision makers.

The corresponding value function $V(\pi) : \mathfrak{S} \rightarrow \mathfrak{R}$ is defined as the cumulative discounted reward achieved by following the actions prescribed by the policy π when starting from a specific initial state. Additionally, the action value function $Q^\pi(s, a)$ is introduced to represent the expected cumulative reward when taking action a in state s , considering that the policy π is being followed. This can be expressed as follows:

$$V^\pi(s) = \mathbb{E}[Q^\pi(s, \mathfrak{A}) | \mathfrak{A} \sim \pi(\cdot|s)], \quad (27)$$

$$\begin{aligned} Q^\pi(s, a) &= \mathbb{E}\left[\sum_{t=0}^{\infty} \gamma^t \cdot \mathfrak{R}_t | \mathfrak{S}_0 = s, \mathfrak{A}_0 = a\right] \\ &= r(s, a) + \gamma \mathbb{E}[V^\pi(\mathfrak{S}') | \mathfrak{S}' \sim \mathfrak{P}(\cdot|s, a)], \end{aligned} \quad (28)$$

where, \mathfrak{R}_t represents the immediate reward obtained at time t , and γ (where $0 < \gamma < 1$) denotes the discount factor applied in the computation of future rewards. The discount factor determines the weight of future rewards in the decision-making process.

Exploring the dynamics of the environment, especially when accounting for variable channel conditions and calculating transition probabilities, is a highly complex task. Determining the value function in such scenarios presents a significant

challenge. To address MDPs, two primary strategies are employed: model-based and model-free approaches. In instances where there is uncertainty surrounding transition probabilities and reward functions, the model-free approach of Q-learning proves invaluable for solving the MDP [38].

2) *Deep-Q-Network Algorithm*: In our considered problem, we face the challenge of managing the states space (\mathcal{S}) and actions space (\mathcal{A}) that are inherently high-dimensional and complex. This complexity arises from continuous variable like transmission power, as well as the substantial number of UEs and PRB resources. Traditional Q-learning methods struggle in such scenarios, as many state-action pairs are rarely encountered, leading to inefficient learning processes [35], [38].

To overcome this challenge, we turn to the Deep Q-Network (DQN) approach to tackle our resource allocation problem and optimize parameters such as transmission power, alpha, and beta. DQN offers distinct advantages in handling these complex, high-dimensional state-action spaces by utilizing a deep neural network to approximate the Q -function. DQN's capacity to generalize from prior experiences and its use of techniques such as experience replay and target networks make it an apt choice for addressing resource allocation challenges within our problem domain.

DQN employs experience replay to store into replay memory (\mathcal{M}) and sample transitions from the memory ($\mathcal{S}_t, \mathcal{A}_t, \mathcal{R}_t, \mathcal{S}_{t+1}$) to train the neural network with stochastic gradient descent. This method helps acquire uncorrelated samples from a temporally correlated MDP trajectory, enhancing gradient estimation accuracy. A target network Q_{θ^*} is also used, where independent samples are obtained from the replay memory. These samples are used to update the Q -network's parameter, improving learning stability and efficiency [38]. We compute the target value and update θ by the gradient of equations 29-30.

$$Y = \mathfrak{R}(s, a) + \gamma \max_{a' \in \mathcal{A}} Q_{\theta^*}(s', a'), \quad (29)$$

$$L(\theta) = \|Y - Q_{\theta}(s, a)\|^2, \quad (30)$$

The parameter θ^* is updated every T_{target} steps by setting it equal to θ . The target network remains unchanged for T_{target} steps and is then updated using the current weights of the Q-network.

Our DQN training employs the epsilon-greedy policy for action selection. This means that the agent chooses the action with the highest Q-value with a probability of $1 - \epsilon$, and with a probability of ϵ , it explores and selects a random action. The policy function is represented as:

$$\pi(S) = \begin{cases} \operatorname{argmax}_a Q(\mathcal{S}, a) & \text{with probability } 1 - \epsilon \\ \text{random action} & \text{with probability } \epsilon \end{cases}$$

It's worth noting that the complete training algorithm for DQN is detailed in [38], and for our specific problem, we have utilized Algorithm 3 for training the DQN model.

C. Proposed Method

In recent times, DL techniques have found application in enhancing the accuracy and efficiency of resource allocation

and transmission power control in wireless communication systems, as demonstrated in several studies [39]–[42]. These approaches excel in learning complex, non-linear relationships between input features like channel matrices and output decisions, such as power and resource allocation. What distinguishes DL-based resource allocation is its ability to effectively manage the dynamic and intricate nature of wireless communication systems. These approaches can adapt to varying channel conditions and UE, resulting in improved network performance compared to traditional optimization methods.

In our proposed DL-based resource allocation method, we feed the channel matrix into a DNN. This network is responsible for learning optimal resource allocation decisions that adhere to network constraints while maximizing the defined objective function (weighted aggregated data rate). We also employ a flattened vector with dimensions UB , derived from the channel gain matrix, as input for a machine-learning model, which includes a VAE. This autoencoder utilizes the channel matrix to generate the power vector. The key innovation in our approach is the introduction of contrastive loss as an additional term in the VAE's loss function. This addition refines the learning of representations, significantly enhancing the accuracy of solutions to resource allocation problems. Subsequent sections will provide a detailed exploration of each component in our proposed method.

1) *Variational Autoencoder*: The VAE is a specific type of generative model frequently applied in unsupervised learning tasks. It functions as a DNN designed to generate new data samples resembling a provided set of training data. Utilizing a VAE confers a notable advantage: it adeptly captures the intrinsic distribution of the channel gain matrix. This acquired knowledge proves immensely valuable when confronting the resource allocation problem [43].

In a VAE, let's denote the input data as x , a latent variable representing a lower-dimensional data representation as z , and $p_{\theta}(x)$ as a generative model representing the data distribution based on the latent variable. The primary goal of a VAE is to maximize the likelihood of the data given the model parameters, denoted as θ . This likelihood can be mathematically expressed as:

$$\log p_{\theta}(x) = \mathbb{E}_{q_{\phi}(z|x)}[\log p_{\theta}(x|z)] - D_{KL}(q_{\phi}(z|x)|p(z)), \quad (31)$$

where, $q_{\phi}(z|x)$ corresponds to the encoder network, which models the posterior distribution of the latent variable given the input data. The term $D_{KL}(q_{\phi}(z|x)|p(z))$ represents the Kullback-Leibler (KL) divergence between this posterior distribution and the prior distribution of the latent variable.

The objective function can be enhanced by adjusting the parameters of both the generative model, denoted as θ , and the encoder network, represented as ϕ . This optimization process involves iteratively updating these parameters and computing the gradient of the objective concerning them, as outlined in [43]. Fig. 3 illustrates the VAE architecture tailored for addressing the resource allocation and network slicing problem.

To provide a more detailed explanation, a VAE comprises two primary components: an encoder and a decoder. The

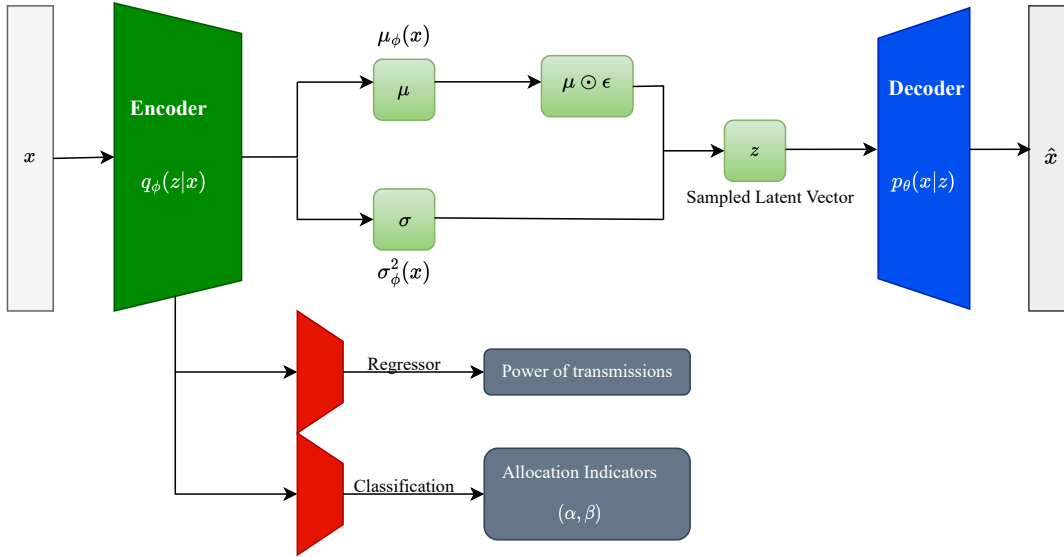


Fig. 3: The architecture of proposed VAE.

encoder accepts the channel gain matrix as input and transforms it into a lower-dimensional representation known as a latent code. Subsequently, the decoder takes this latent code as input and produces an estimation of the transmission power. These two components work in tandem during training to minimize a reconstruction loss. This loss metric quantifies the disparity between the actual transmission power and the predicted transmission power, guiding the network to generate more accurate power predictions.

Using a VAE for resource allocation offers several distinct advantages. Firstly, VAEs exhibit remarkable flexibility, enabling them to model intricate distributions. This characteristic is particularly advantageous for capturing the complex and non-linear relationship between channel gains and transmission powers. Secondly, VAEs excel at discerning the underlying structure within data, enabling them to make informed predictions even when confronted with previously unseen data [44]. Thirdly, the latent code generated by the encoder serves as a compressed representation of channel gains, which can be leveraged for diverse tasks like visualization, clustering, and anomaly detection.

Moreover, resource allocation problems are inherently non-convex and can be exceptionally challenging when using traditional optimization approaches. The introduction of VAEs provides a more versatile and effective means of tackling these intricate problems.

Our dataset comprises a total of Q training samples, divided into two categories: Q_L labeled samples and Q_U unlabeled samples. These samples are represented by pairs of channel matrices and their corresponding power allocation vectors, denoted as H_i and Γ_i for labeled samples (where i ranges from 1 to Q_L), and H_j for unlabeled samples (where j ranges from 1 to Q_U).

It is important to note that the process of generating these input channel matrices is computationally less intensive compared to traditional methods, as documented in previous research [45].

To train the supervised learning component of our algorithm, we employ the ADAM optimizer [46]. This optimizer facilitates the end-to-end training of the VAE using the Q_L labeled samples. The loss function for the regression problem with ADAM optimization is formulated using the mean squared error (MSE) loss function, defined as follows:

$$L_{supervised} = \frac{1}{\beta_L} \sum_{i \in \beta_L} \|VAE(H_i) - \Gamma_i\|^2. \quad (32)$$

In our resource allocation challenge, the correlation between the xApps dealing with power estimation and the PRBs allocation emerges from their shared foundation within the VAE framework. The VAE operates as a unifying space where both xApps converge, enabling a synergistic exploration and consideration of the pertinent features relevant to both power transmission and PRB allocations. Through this shared space, the xApps gain access to a common latent representation of the channel gain matrices. This shared understanding facilitates a cohesive analysis where the interdependencies between power estimation and PRB allocations are thoroughly examined, allowing for the simultaneous consideration of the critical features that impact both domains. This integration of information aids in making more comprehensive and informed resource allocation decisions, as it ensures that both xApps leverage a unified understanding of the underlying data to optimize their respective objectives. This coordination is pivotal, as it allows for a coordinated and synchronized approach to resource allocation within the O-RAN architecture.

2) *Contrastive Loss*: Contrastive loss is a widely-used loss function in ML for various representation learning tasks, including image or text classification. Its fundamental aim is to construct a representation of data points that encourages similar data points to be closer together in the representation space while simultaneously pushing dissimilar data points farther apart [17].

Mathematically, the contrastive loss can be expressed as follows:

$$L = \frac{1}{2N} \sum_{i=1}^N (y_i \cdot d^2(\mathbf{x}_i, \mathbf{x}_i^+) + (1 - y_i) \cdot \max(0, m - d^2(\mathbf{x}_i, \mathbf{x}_i^-))), \quad (33)$$

where N is the number of data points, \mathbf{x}_i is the representation of the i^{th} data point, \mathbf{x}_i^+ and \mathbf{x}_i^- are the representations of the similar and dissimilar data points respectively, y_i is a binary label indicating whether \mathbf{x}_i and \mathbf{x}_i^+ are similar or dissimilar, and $d(\mathbf{x}_i, \mathbf{x}_i^+)$ is the distance function between \mathbf{x}_i and \mathbf{x}_i^+ . The parameter m is a margin that separates the similar and dissimilar representations.

To use contrastive loss in our resource allocation problem, we need to create similar and dissimilar channel gain matrices. One way to create channel gain matrices that are either similar or dissimilar is by using a statistical model of the channel that captures the relevant properties of the communication environment. The Rayleigh fading model is a commonly used statistical model for wireless channels, which assumes that the channel gain is a complex Gaussian random variable with zero mean and a variance that depends on the distance between the transmitter and receiver [47], [48].

To create similar channel gain matrices, coefficients with similar magnitude and phase can be generated. Conversely, to create dissimilar channel gain matrices, coefficients with different magnitude and phase can be generated by introducing randomness into the channel model by using a Rayleigh fading model. To generate a channel gain matrix using this model, a matrix of complex Gaussian random variables with zero mean and a variance that depends on the distance between the transmitter and receiver can be generated as well as considering the interference as noise [49], [50]. The variance can be adjusted to create similar or dissimilar channel gain matrices based on the desired level of correlation between the channels. The mathematical formulation of this approach can be expressed as:

$$\mathbf{H}_{noise} = \mathbf{H} + \epsilon, \quad (34)$$

where \mathbf{H}_{noise} is the channel gain matrix with added noise, \mathbf{H} is the original channel gain matrix, and ϵ is a Gaussian noise matrix with zero mean and standard deviation σ .

Once we have created similar and dissimilar channel gain matrices, we can train our contrastive loss function using these matrices as inputs. The loss function can be formulated as:

$$L_{Contrastive}(\theta) = \frac{1}{\beta_L} \sum_{i \in \beta_L} \left[-\log \frac{\exp \frac{f(\underline{H}_i)^T \times f(\underline{H}_i)}{\tau}}{\exp \frac{f(\underline{H}_i)^T \times f(\underline{H}_i)}{\tau} + \sum_{i \neq j} \exp \frac{f(\underline{H}_i)^T \times f(\underline{H}_j)}{\tau}} \right], \quad (35)$$

where θ is the set of parameters in the variational autoencoder model, τ is a temperature hyperparameter and $L(\theta)$ is the contrastive loss function. \underline{H}_i and \bar{H}_i are the similar matrices to the the main channel gain matrix (H_i), which allow us to train our proposed model [51]. By minimizing this loss function, we can learn a set of parameters that enable our model

to differentiate between similar and dissimilar channel gain matrices and produce a power control decision that optimizes the network performance.

3) *Training the proposed model:* In this section, we will describe the training phase of our proposed method, which consists of two parts: the supervised learning part, where the VAE is trained to regress the power transmission, and the unsupervised learning part, where the contrastive loss is used to improve the generalization and robustness of our proposed method. There are several key parameters that should be taken into consideration in training the supervised part. The latent space dimension represents the size of the hidden representation learned by the VAE [45]. A larger latent space dimension can lead to a more expressive model, but also increases the risk of overfitting. The learning rate determines the speed at which the model learns from the data. The batch size determines the number of samples used for each iteration of the training process. The number of epochs determines the number of times the model will be trained on the data. $L1$ and $L2$ regularization to prevent overfitting by adding a penalty term to the loss function of supervised learning [52]. The proposed model is developed using the PyTorch [53] software framework. Both validation size and test size are 20% of the dataset, allowing for a more thorough evaluation of the proposed model's performance. Hyper-parameter tuning yields the value of hyperparameters, which can be found in the Table III.

The initial model was pre-trained through self-supervised learning, using unlabeled channel gain matrices that corresponded to the stated loss function. The pre-training was based on regression loss. After pre-training, the DL model was fine-tuned for power transmission regression using the proposed method. The performance of the trained model was evaluated on test data points using various performance metrics, while the number of labeled training channel gain matrices were varied. Additionally, a supervised baseline performance for the regression task was obtained by training the DL model with all available labeled training channel gain matrices.

4) *Performance Metrics:* The performance metrics for evaluating our proposed method are Mean Absolute Error (MAE), cosine similarity, and correlation. MAE measures the average absolute difference between the predicted values and the actual values. Cosine similarity measures the similarity between two vectors in a multi-dimensional space. The Pearson correlation (R) represents the amount of variation in the output-dependent attribute that can be predicted by the input-independent variable. It also provides insight into how accurately a model can predict outcomes based on how much of the variation in those outcomes can be explained by the input-independent variable. They can be calculated as follows:

$$MAE = \frac{1}{N} \sum_{i=1}^N |y_i - \hat{y}_i|, \quad (36)$$

$$Cosine-Similarity(Y, \hat{Y}) = \frac{Y \cdot \hat{Y}}{|Y| |\hat{Y}|}, \quad (37)$$

$$correlation(\hat{Y}, Y) = \frac{cov(\hat{Y}, Y)}{\sigma_{\hat{Y}} \sigma_Y}, \quad (38)$$

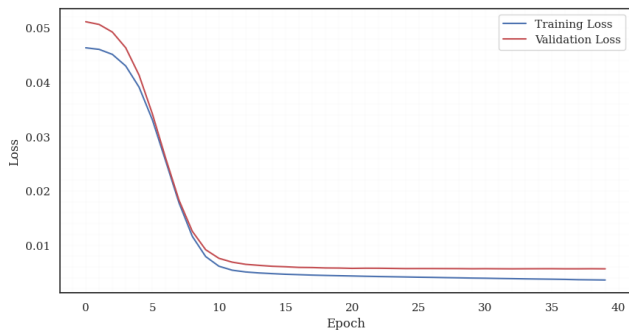


Fig. 4: Loss values of training and validation dataset.

where N is the total number of samples, y_i is the true value, and \hat{y}_i is the predicted value, and \cdot represents the dot product, and $|\cdot|$ represents the magnitude of a vector. As for correlation, $\text{cov}(\hat{Y}, Y)$ is the covariance between the predicted value and the true value, and $\sigma_{\hat{Y}}$ and σ_Y are the standard deviations of the variables.

V. SIMULATION RESULTS

In the following subsections, we will begin by analyzing the initial values to simulate the proposed algorithm. Subsequently, we will compare the results obtained using SS-VAE with those from ESA and DQN. This comparative analysis aims to assess the accuracy and effectiveness of our proposed DL model in addressing the resource allocation problem.

A. Initial points and performance of training the model

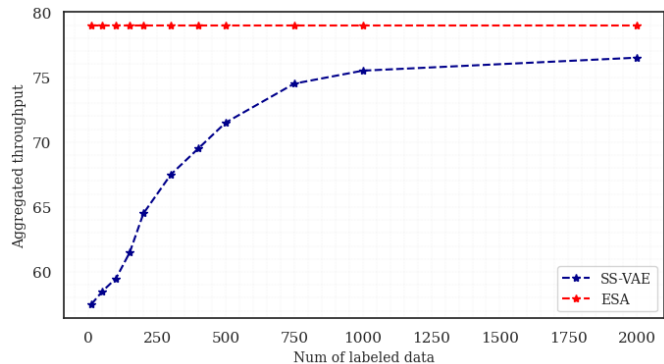
In this section, we present numerical results for the considered resource allocation problem to evaluate the performance of our proposed model (SS-VAE) compared to state-of-the-art methods, namely ESA and DQN. The initial values and parameters used to run and simulate our proposed algorithm (SS-VAE) and the benchmark algorithms (ESA and DQN) are provided in Table I, Table II, and Table III.

As previously discussed, our proposed model aims to estimate the transmission power corresponding to each input channel matrix. These estimated power values, derived from the weights of the VAE, are then used to predict the allocation indicators $(\alpha_{u,b,s}, \beta_{u,b,m,s})$. To streamline the training process, it is crucial to convert the dimensions of each channel matrix data into a one-dimensional vector. More specifically, our model takes as input a flattened UB -dimensional vector obtained from the channel gain matrix.

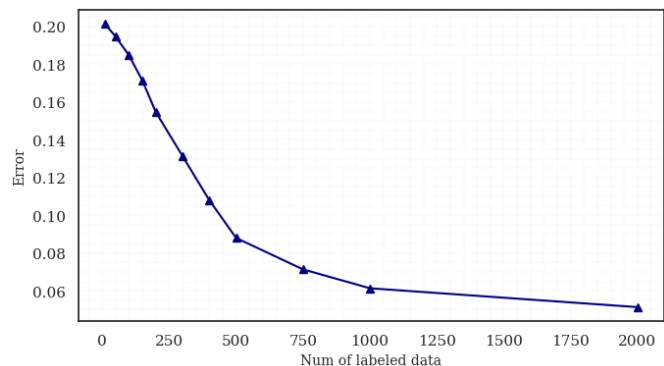
The loss values for both the validation and training data points is depicted in Fig. 4.

The decreasing trend of loss values illustrate that the proposed method (SS-VAE) could accurately estimate the target values (power of transmission, association indicators). In fact, the model can map the input channel gain matrix to the power of transmission as well as the indicators by employing the VAE's property in learning the underlying information.

The performance metrics for the test data, as presented in Table IV, clearly indicate that our proposed method (SS-VAE), which estimates transmission power based on the input



(a) Agg. throughput vs. Number of labeled data.



(b) Association Error vs. Number of labeled data.

Fig. 5: Comparison of the algorithms (SS-VAE vs. ESA).

channel gain matrix, exhibits the best generalization. This improvement can be attributed to the utilization of VAE, which has been proven to enhance generalization in various related tasks. In addition, the pre-training method involving the contrastive loss has further enhanced our model's capacity to learn the underlying features, ultimately reducing generalization errors.

The R^2_{Score} value for the test data indicates that our model successfully explains a significant portion of the variance in estimating the power of transmissions. This suggests that a substantial proportion of the variability in the dependent variable (power of transmissions) can be accounted for by the independent variables (the channel gain matrix) integrated into the model. In simpler terms, the model is effective at describing and understanding the variations in the data, especially in terms of transmission power.

B. Comparison of the algorithms

In the next phase, we will assess the performance of our proposed SS-VAE method by comparing it to the ESA algorithm. This evaluation will specifically consider the impact of the number of labeled samples used for training the supervised part of SS-VAE, as illustrated in Fig. 5.

We analyze the aggregated throughput under varying numbers of labeled data points, as generated by our proposed SS-VAE algorithm and the ESA. As depicted in Fig. 5a, our proposed model achieves a similar aggregated throughput when

TABLE I: Resource Allocation Simulation Parameters

Parameter	Value
Noise power	-174 dBm
bandwidth of each sub-carrier	180 KHz
Maximum transmit power of each O-RU	40 dBm
Maximum fronthaul capacity	46 bps
Maximum data rate for eMBB	20 bps
Maximum data rate for URLLC	2 bps
Maximum power for URLLC & eMBB	30 dBm

TABLE II: DQN Training Parameters

Number of episodes and steps	250, 50
$\gamma, \epsilon_{finalvalue}, \epsilon_{decayfactor}$	0.9, 0.1, 0.9995
Replay memory size	400

TABLE IV: Performance metrics of the proposed model

Performance Metric	MAE	R^2_{Score}	Cosine Similarity
Value	0.09207532	0.76795106	0.988023

compared to the ESA. Moreover, the discrepancy between our model and the ESA decreases significantly as the number of labeled data points increases.

We further evaluate the performance of the SS-VAE model and ESA in terms of binary variables related to user association ($\alpha_{u,b,s}$) and PRB allocation ($\beta_{u,b,m,s}$). Fig. 5b displays the ratio of the absolute sum of differences in these binary variables between the SS-VAE and ESA to the total number of them ($\frac{|\alpha_{ESA} - \alpha_{SS-VAE}| + |\beta_{ESA} - \beta_{SS-VAE}|}{\# \text{ Number of } (\alpha \& \beta)}$), as the number of labeled channel gain matrices (data points) increases. Notably, the difference between the $L1 - norm$ of binary variables obtained by the SS-VAE method significantly decreases in comparison to ESA as the number of labeled data points grows.

The results above highlight the reliable performance of our proposed method (SS-VAE) in estimating transmission powers, user association, and PRB allocation when compared to the ESA. In the subsequent section, we will assess its performance under different initial conditions, varying the number of slices, UEs, and thresholds for transmission power and rate. Since the SS-VAE exhibits lower error compared to the ESA but doesn't perform identically in the resource allocation problem, we will also evaluate its performance alongside another benchmark algorithm, the aforementioned DQN algorithm in Section IV-B. DQN has demonstrated practical and valuable results in resource allocation problems within wireless networks and similar domains, enabling us to assess the robustness of our proposed algorithm.

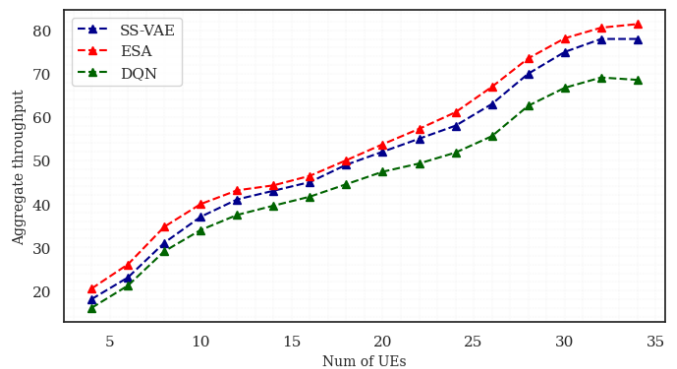
C. Performance results

In this section, we will assess the performance of the proposed model (SS-VAE) in the resource allocation problem under various scenarios. To begin, we will examine the aggregate weighted rate in relation to the number of UEs using three different algorithms: SS-VAE, ESA, and DQN, as depicted in Fig. 6.

Fig. 6a demonstrates that the proposed approach (SS-VAE) exhibits a performance that is comparable to the ESA. There

TABLE III: Proposed Model Training Parameters

Type	Training Parameter	Value
Optimizer	Initial learning rate	0.001
	β_1	0.99
	β_2	0.99
	Weight Decay	0.9
Model	Number of encoding layer	20
	Dimension of latent space	20
	Contrastive loss temperature	0.25
	Activation Function	ReLU
	Dropout Rate	0.3
Training	Epoch	40
	Batch Size	128
	Train/Validation Split	0.2



(a) Aggr. throughput vs. number of UEs.

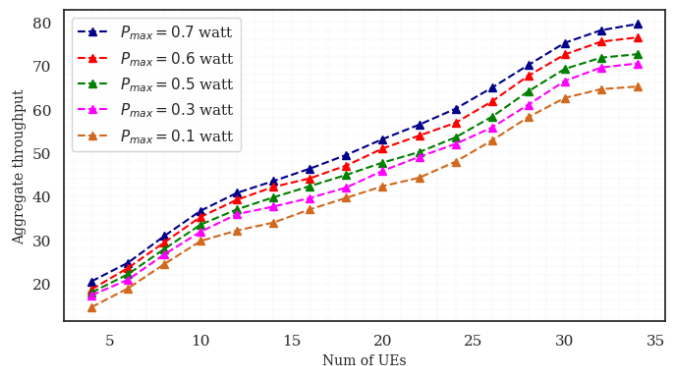
(b) Aggr. throughput vs. number of UEs (P_{O-RU}).

Fig. 6: Aggregated throughput of the SS-VAE vs. Number of UEs.

are no significant differences in terms of aggregated throughput between the two. Additionally, SS-VAE achieves a superior aggregated throughput across all UE numbers when compared to the DQN algorithm. This highlights the robustness and high accuracy of our proposed method for the resource allocation problem. It's worth noting that the sum of data rate increases initially as more UEs join the service for all three examined algorithms. However, it reaches a plateau after 30-35 UEs per service due to power limitations and interference constraints.

Fig. 6b depicts the aggregated throughput achieved by the SS-VAE algorithm concerning different power levels of O-RU and varying numbers of UEs. As per established knowledge

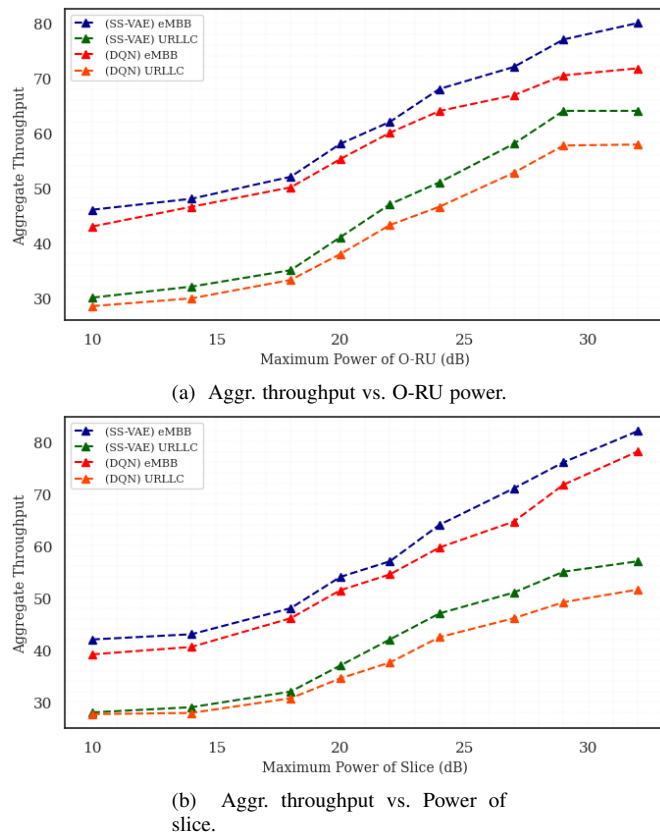


Fig. 7: Aggregated throughput of SS-VAE vs. Power values.

[15], both increasing the power of O-RU and the number of UEs lead to higher aggregated throughput. The highest aggregated throughput is observed when the power of O-RU is at its highest.

Fig. 7 displays the aggregated throughput for two specified service types (eMBB and URLLC), which has been obtained using the SS-VAE and DQN algorithms, in relation to the power values. This presentation aims to evaluate the performance of our proposed algorithm for these services in comparison to a benchmark algorithm.

Fig. 7 displays the aggregated throughput for the two considered service types, namely eMBB and URLLC, as determined by the SS-VAE and DQN algorithms. This visualization is intended to evaluate the performance of our proposed algorithm (SS-VAE) for these services in comparison to a benchmark algorithm.

Fig. 7a depicts the influence of O-RU's maximum power thresholds on the aggregate weighted rate for both eMBB and URLLC services, comparing two algorithms, SS-VAE and DQN. The results indicate a direct correlation between increased maximum power and higher weighted rates. Additionally, the SS-VAE algorithm consistently outperforms the DQN algorithm, achieving higher aggregated throughput for both service types across various power values.

Similarly, in Fig. 7b, variations in total data rates are displayed concerning the maximum power for distinct cases of eMBB and URLLC services. The results reveal a direct increase in data rates as the maximum power of each UE in dif-

ferent service instances rises. Notably, the SS-VAE algorithm consistently outperforms the DQN algorithm, securing higher aggregated throughput for both service types across various power threshold values.

VI. CONCLUSION

In this paper, a novel model is introduced for the O-RAN system's downlink, aiming to coordinate multiple independent xAPPs to tackle the resource allocation problem with network slicing in the O-RAN architecture. This problem is addressed for two specific 5G services, namely eMBB and URLLC, with the overarching objective of optimizing the aggregate weighted rate by managing RU associations, power allocation, and PRBs.

Due to the non-convex and NP-hard nature of the resource allocation optimization problem, we introduced a semi-supervised learning approach as an efficient solution for UE and PRB allocation. Our two-step algorithm starts by reformulating the problem into an optimization problem considering the objective function and constraints. The second step consists of a two-part training process: firstly, supervised learning employing a VAE to estimate power transmission regression and association indicators, and then unsupervised learning with a contrastive loss approach, enhancing the model's generalization and robustness.

To evaluate our proposed algorithm's performance, we conducted comparisons with benchmark algorithms ESA and DQN across various scenarios. The results indicate that our approach achieves a rate similar to ESA while outperforming the DQN algorithm, highlighting its effectiveness. We further explore different scenarios tailored to each service, eMBB and URLLC, considering their unique QoS requirements. Through simulations, we demonstrate the superior efficiency of our model, particularly in terms of sample efficiency, making it a compelling solution for resource allocation challenges within the O-RAN system.

In future research, we plan to explore several areas. Firstly, we intend to evaluate the end-to-end delay experienced by individual UEs and investigate the impact of deployment costs associated with network function placement tackle. Furthermore, addressing UE mobility is crucial in practical scenarios. In addition, we will explore alternative ML and optimization algorithms to improve our resource allocation approach, providing new research avenues in this dynamic field.

REFERENCES

- [1] L. M. Larsen, A. Checko, and H. L. Christiansen, "A survey of the functional splits proposed for 5G mobile crosshaul networks," *IEEE Communications Surveys & Tutorials*, vol. 21, no. 1, pp. 146–172, 2018.
- [2] O. Nassef, W. Sun, H. Purmehdi, M. Tatipamula, and T. Mahmoodi, "A survey: Distributed machine learning for 5g and beyond," *Computer Networks*, vol. 207, p. 108820, 2022.
- [3] C.-X. Wang, X. You, X. Gao, X. Zhu, Z. Li, C. Zhang, H. Wang, Y. Huang, Y. Chen, H. Haas *et al.*, "On the road to 6g: Visions, requirements, key technologies and testbeds," *IEEE Communications Surveys & Tutorials*, 2023.
- [4] M. K. Shehzad, L. Rose, M. M. Butt, I. Z. Kovács, M. Assaad, and M. Guizani, "Artificial intelligence for 6g networks: Technology advancement and standardization," *IEEE Vehicular Technology Magazine*, vol. 17, no. 3, pp. 16–25, 2022.

- [5] "O-RAN: Towards an Open and Smart RAN, O-RAN Alliance White Paper, October 2018, O-RAN Alliance."
- [6] S. Zhang, "An overview of network slicing for 5g," *IEEE Wireless Communications*, vol. 26, no. 3, pp. 111–117, 2019.
- [7] A. S. Abdalla, P. S. Upadhyaya, V. K. Shah, and V. Marojevic, "Toward next generation open radio access networks: What o-ran can and cannot do!" *IEEE Network*, vol. 36, no. 6, pp. 206–213, 2022.
- [8] L. Tang, "Multi-dimensional resource allocation algorithm for end-to-end network slicing," 2023.
- [9] A. Oliveira and T. Vazão, "Towards green machine learning for resource allocation in beyond 5g ran slicing," *Computer Networks*, p. 109877, 2023.
- [10] P. Popovski, K. F. Trillingsgaard, O. Simeone, and G. Durisi, "5g wireless network slicing for embb, urllc, and mmhc: A communication-theoretic view," *Ieee Access*, vol. 6, pp. 55 765–55 779, 2018.
- [11] J. Huang, F. Yang, C. Chakraborty, Z. Guo, H. Zhang, L. Zhen, and K. Yu, "Opportunistic capacity based resource allocation for 6g wireless systems with network slicing," *Future Generation Computer Systems*, vol. 140, pp. 390–401, 2023.
- [12] M. Al-Ali and E. Yaacoub, "Resource allocation scheme for embb and urllc coexistence in 6g networks," *Wireless Networks*, pp. 1–20, 2023.
- [13] "Deploying 5G networks, 2020, Nokia corporation. Available at: <https://www.nokia.com/networks/5g/mobile/5g-resources/>."
- [14] L. Bonati, S. D'Oro, M. Polese, S. Basagni, and T. Melodia, "Intelligence and learning in o-ran for data-driven nextg cellular networks," *IEEE Communications Magazine*, vol. 59, no. 10, pp. 21–27, 2021.
- [15] M. K. Motalleb, V. Shah-Mansouri, S. Parsaeefard, and O. L. A. López, "Resource allocation in an open ran system using network slicing," *IEEE Transactions on Network and Service Management*, vol. 20, no. 1, pp. 471–485, 2022.
- [16] L. Feng, Y. Zi, W. Li, F. Zhou, P. Yu, and M. Kadoch, "Dynamic resource allocation with ran slicing and scheduling for urllc and embb hybrid services," *Ieee Access*, vol. 8, pp. 34 538–34 551, 2020.
- [17] T. Chen, S. Kornblith, M. Norouzi, and G. Hinton, "A simple framework for contrastive learning of visual representations," in *International conference on machine learning*. PMLR, 2020, pp. 1597–1607.
- [18] D. P. Kingma and M. Welling, "Auto-encoding variational bayes," *arXiv preprint arXiv:1312.6114*, 2013.
- [19] M. K. Motalleb, V. Shah-Mansouri, and S. N. Naghadeh, "Joint power allocation and network slicing in an open ran system," *arXiv preprint arXiv:1911.01904*, 2019.
- [20] N. Kazemifard and V. Shah-Mansouri, "Minimum delay function placement and resource allocation for open ran (o-ran) 5g networks," *Computer Networks*, vol. 188, p. 107809, 2021.
- [21] C. Benzaïd, T. Taleb, A. Sami, and O. Hireche, "Fortisedos: A deep transfer learning-empowered economical denial of sustainability detection framework for cloud-native network slicing," *IEEE Transactions on Dependable and Secure Computing*, 2023.
- [22] C. Benzaïd, T. Taleb, and J. Song, "Ai-based autonomic and scalable security management architecture for secure network slicing in b5g," *IEEE Network*, vol. 36, no. 6, pp. 165–174, 2022.
- [23] Y. Azimi, S. Yousefi, H. Kalbhani, and T. Kunz, "Applications of machine learning in resource management for ran-slicing in 5g and beyond networks: A survey," *IEEE Access*, vol. 10, pp. 106 581–106 612, 2022.
- [24] C. Bektas, D. Overbeck, and C. Wietfeld, "Samus: Slice-aware machine learning-based ultra-reliable scheduling," in *ICC 2021-IEEE International Conference on Communications*. IEEE, 2021, pp. 1–6.
- [25] J. Li, X. Zhang, J. Zhang, J. Wu, Q. Sun, and Y. Xie, "Deep reinforcement learning-based mobility-aware robust proactive resource allocation in heterogeneous networks," *IEEE Transactions on Cognitive Communications and Networking*, vol. 6, no. 1, pp. 408–421, 2019.
- [26] W. Wu, N. Chen, C. Zhou, M. Li, X. Shen, W. Zhuang, and X. Li, "Dynamic ran slicing for service-oriented vehicular networks via constrained learning," *IEEE Journal on Selected Areas in Communications*, vol. 39, no. 7, pp. 2076–2089, 2020.
- [27] J. A. Ayala-Romero, A. Garcia-Saavedra, M. Gramaglia, X. Costa-Perez, A. Banchs, and J. J. Alcaraz, "vrain: Deep learning based orchestration for computing and radio resources in vrans," *IEEE Transactions on Mobile Computing*, vol. 21, no. 7, pp. 2652–2670, 2020.
- [28] X. Wang, J. D. Thomas, R. J. Piechocki, S. Kapoor, R. Santos-Rodríguez, and A. Parekh, "Self-play learning strategies for resource assignment in open-ran networks," *Computer Networks*, vol. 206, p. 108682, 2022.
- [29] A. Ndikumana, K. K. Nguyen, and M. Cheriet, "Federated learning assisted deep q-learning for joint task offloading and fronthaul segment routing in open ran," *IEEE Transactions on Network and Service Management*, 2023.
- [30] S. Samarakoon, M. Bennis, W. Saad, and M. Debbah, "Federated learning for ultra-reliable low-latency v2v communications," in *2018 IEEE global communications conference (GLOBECOM)*. IEEE, 2018, pp. 1–7.
- [31] M. Elsayed and M. Erol-Kantarci, "Reinforcement learning-based joint power and resource allocation for urllc in 5g," in *2019 IEEE Global Communications Conference (GLOBECOM)*. IEEE, 2019, pp. 1–6.
- [32] T. Erpek, A. Abdelhadi, and T. C. Clancy, "An optimal application-aware resource block scheduling in lte," in *2015 International Conference on Computing, Networking and Communications (ICNC)*. IEEE, 2015, pp. 275–279.
- [33] H. Eiselt, C.-L. Sandblom *et al.*, *Nonlinear optimization*. Springer, 2019.
- [34] J. Nocedal and S. J. Wright, *Numerical optimization*. Springer, 1999.
- [35] A. Filali, B. Nour, S. Cherkaoui, and A. Kobbane, "Communication and computation o-ran resource slicing for urllc services using deep reinforcement learning," *IEEE Communications Standards Magazine*, vol. 7, no. 1, pp. 66–73, 2023.
- [36] A. Feriani and E. Hossain, "Single and multi-agent deep reinforcement learning for ai-enabled wireless networks: A tutorial," *IEEE Communications Surveys & Tutorials*, vol. 23, no. 2, pp. 1226–1252, 2021.
- [37] K. Suh, S. Kim, Y. Ahn, S. Kim, H. Ju, and B. Shim, "Deep reinforcement learning-based network slicing for beyond 5g," *IEEE Access*, vol. 10, pp. 7384–7395, 2022.
- [38] J. Fan, Z. Wang, Y. Xie, and Z. Yang, "A theoretical analysis of deep q-learning," in *Learning for dynamics and control*. PMLR, 2020, pp. 486–489.
- [39] V. Lima, M. Eisen, K. Gatsis, and A. Ribeiro, "Resource allocation in large-scale wireless control systems with graph neural networks," *IFAC-PapersOnLine*, vol. 53, no. 2, pp. 2634–2641, 2020.
- [40] P. E. Iturria-Rivera, H. Zhang, H. Zhou, S. Mollahasani, and M. Erol-Kantarci, "Multi-agent team learning in virtualized open radio access networks (o-ran)," *Sensors*, vol. 22, no. 14, p. 5375, 2022.
- [41] N. Hammami and K. K. Nguyen, "On-policy vs. off-policy deep reinforcement learning for resource allocation in open radio access network," in *2022 IEEE Wireless Communications and Networking Conference (WCNC)*. IEEE, 2022, pp. 1461–1466.
- [42] Q. Wang, Y. Liu, Y. Wang, X. Xiong, J. Zong, J. Wang, and P. Chen, "Resource allocation based on radio intelligence controller for open ran towards 6g," *IEEE Access*, 2023.
- [43] D. P. Kingma, M. Welling *et al.*, "An introduction to variational autoencoders," *Foundations and Trends® in Machine Learning*, vol. 12, no. 4, pp. 307–392, 2019.
- [44] U. Jain, Z. Zhang, and A. G. Schwing, "Creativity: Generating diverse questions using variational autoencoders," in *Proceedings of the IEEE conference on computer vision and pattern recognition*, 2017, pp. 6485–6494.
- [45] Q. Shi, M. Razaviyayn, Z.-Q. Luo, and C. He, "An iteratively weighted mmse approach to distributed sum-utility maximization for a mimo interfering broadcast channel," *IEEE Transactions on Signal Processing*, vol. 59, no. 9, pp. 4331–4340, 2011.
- [46] D. P. Kingma and J. Ba, "Adam: A method for stochastic optimization," *arXiv preprint arXiv:1412.6980*, 2014.
- [47] A. Grant, "Rayleigh fading multi-antenna channels," *EURASIP Journal on Advances in Signal Processing*, vol. 2002, pp. 1–14, 2002.
- [48] A. J. Goldsmith and S.-G. Chua, "Adaptive coded modulation for fading channels," *IEEE Transactions on communications*, vol. 46, no. 5, pp. 595–602, 1998.
- [49] C. Geng, N. Naderializadeh, A. S. Avestimehr, and S. A. Jafar, "On the optimality of treating interference as noise," *IEEE Transactions on Information Theory*, vol. 61, no. 4, pp. 1753–1767, 2015.
- [50] N. Naderializadeh and A. S. Avestimehr, "Itlinq: A new approach for spectrum sharing in device-to-device communication systems," *IEEE journal on selected areas in communications*, vol. 32, no. 6, pp. 1139–1151, 2014.
- [51] N. Naderializadeh, "Contrastive self-supervised learning for wireless power control," in *ICASSP 2021-2021 IEEE International Conference on Acoustics, Speech and Signal Processing (ICASSP)*. IEEE, 2021, pp. 4965–4969.
- [52] K. Janocha and W. M. Czarnecki, "On loss functions for deep neural networks in classification," *arXiv preprint arXiv:1702.05659*, 2017.

- [53] A. Paszke, S. Gross, F. Massa, A. Lerer, J. Bradbury, G. Chanan, T. Killeen, Z. Lin, N. Gimeshin, L. Antiga *et al.*, “Pytorch: An imperative style, high-performance deep learning library,” *Advances in neural information processing systems*, vol. 32, 2019.